Palaeogeography, Palaeoclimatology, Palaeoecology 516 (2019) 54–63

Contents lists available at ScienceDirect

Palaeogeography, Palaeoclimatology, Palaeoecology

journal homepage: www.elsevier.com/locate/palaeo

Sclerochronological basis for growth band counting: A reliable technique for life-span determination of *Crassostrea virginica* from the mid-Atlantic United States

Joshua B. Zimmt[a,b,*], Rowan Lockwood[a], C. Fred T. Andrus[c], Gregory S. Herbert[d]

[a] Department of Geology, The College of William and Mary, P.O. Box 8795, Williamsburg, VA 23187, USA
[b] Department of Integrative Biology, University of California, Berkeley, CA 94720, USA
[c] Department of Geological Sciences, University of Alabama, Tuscaloosa, AL 35487, USA
[d] School of Geosciences, University of South Florida, 4202 E. Fowler Avenue, Tampa, FL 33620, USA

ARTICLE INFO

Keywords:
Sclerochronology
Conservation paleobiology
Life history
Stable oxygen isotopes
Oysters

ABSTRACT

Widely used sclerochronological methods for biologically aging fossilized oysters, such as $\delta^{18}O$ and Mg/Ca analyses, are costly, time-consuming, and not always practical for population-level analyses. A method that relies on visible morphological features, such as growth bands, to determine the lifespan of *Crassostrea virginica* would provide a cost-efficient and reliable alternative. Previous studies have assessed whether counting growth bands can be used to biologically age *C. virginica* from the southeastern U.S. but have produced conflicting results. For this study, we conducted subseasonal sclerochronological analyses on Pleistocene *C. virginica* from the mid-Atlantic U.S. to determine whether growth band counting could be used to reliably measure oyster lifespan.

A highly significant correlation exists between $\delta^{18}O$ peaks and major (annual) grey growth bands in these oysters. Major grey and white growth bands differ significantly with respect to $\delta^{18}O$ values. These data suggest that, for *C. virginica* from the Pleistocene of the mid-Atlantic U.S., major grey growth bands are accreted during the colder months of the year and can be used as annual markers to biologically age specimens. The results presented here differ from previous studies that reported no link between growth bands and $\delta^{18}O$ values, possibly because the latter focused on lower latitude regions with different seasonal temperature regimes and sampled only the early stages of growth, which contain morphological features that could be confused with major growth bands. While growth band counting of oysters shows promise as a method for biologically aging oysters that experience high seasonal temperature variability, future studies are needed to assess its applicability over a broader geographic range.

1. Introduction

Understanding the population ecology of the eastern oyster (*Crassostrea virginica)* is critical for remediating estuarine habitats along the eastern coast of North America. Oysters have served as a regional food source since pre-Colonial times and continue to play an important economic and ecological role in mid-Atlantic fisheries (Galtsoff, 1964; Andrus and Crowe, 2000; Coen et al., 2007; Harding et al., 2008; Savarese et al., 2016). During the last two centuries, over-fishing and disease have severely depleted oyster populations in this region (Moore, 1897; Jackson et al., 2001), but the extent to which anthropogenic disturbance has affected population demographics and shell growth rates remains unclear.

Oyster management approaches rely on estimates of life history traits from modern oyster populations; however, these populations are neither healthy nor self-sustaining (Harding et al., 2008; Hanke et al., 2017). Determining the life history traits and population dynamics of oyster reefs that have not been significantly altered by human activities would provide resource managers with accurate ecological baselines for remediation (Jackson et al., 2001; Kraeuter et al., 2007; Harding et al., 2008; Mann et al., 2009a; Mann et al., 2009b). The fossil record of *C. virginica* along the U.S. mid-Atlantic Coastal Plain dates back to the earliest Pleistocene and is a potential source of life history data for healthy and sustainable oyster reefs (Kirby et al., 1998; Dietl and Flessa, 2011), but its usefulness is dependent on the ability to biologically age, or determine the lifespan of, fossil oysters.

* Corresponding author at: Department of Integrative Biology, University of California, Berkeley, 1101 Valley Life Science Building, Berkeley, CA, 94720, USA
E-mail addresses: josh_zimmt@berkeley.edu (J.B. Zimmt), rxlock@wm.edu (R. Lockwood), fandrus@ua.edu (C.F.T. Andrus), gherbert@usf.edu (G.S. Herbert).

https://doi.org/10.1016/j.palaeo.2018.11.029
Received 4 July 2018; Received in revised form 12 November 2018; Accepted 23 November 2018
Available online 29 November 2018
0031-0182/

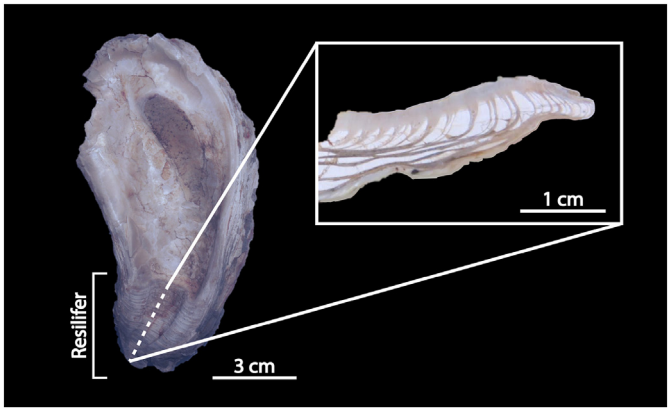

Fig. 1. Interior of the left valve of *C. virginica* specimen AD1 from the Pleistocene of Delaware. The dotted line from the umbo to the interior margin of the resilifer shows the line along which the hinge was bisected. (Inset) Cross-section of the hinge from AD1 mounted in epoxy. Alternating grey and white growth bands are visible in the cross-section.

A combination of shell growth pattern and stable oxygen isotope analyses in bivalves provides a means for studying the ontogeny, life span, and growth rates of individual organisms (Andrus and Crowe, 2008; Goodwin et al., 2010; Andrus and Thompson, 2012; Brocas et al., 2012; Butler and Schöne, 2017; Colonese et al., 2017). Previous sclerochronological studies have sought to correlate morphological features of *Crassostrea* shells to changes in oxygen isotope values for the purpose of estimating lifespan, as *Crassostrea* accretes its shell in isotopic equilibrium with the surrounding water (Hong et al., 1995; Kirby et al., 1998; Andrus and Crowe, 2000; Surge et al., 2001; Fan et al., 2011; Zimmt et al., 2016). Grey and white growth bands within the cross-section of the hinge may have the most potential as growth markers (Fan et al., 2011) (Fig. 1). A correlation among undulations on the hinge surface, grey foliated growth bands in the hinge cross-section, and seasonal $\delta^{18}O$ maxima for *Crassostrea gigas* from the western Bohai Sea (China) was demonstrated using subseasonal sampling (Fan et al., 2011). Such a relationship has been more difficult to establish in *C. virginica*. Kirby et al. (1998) reported a relationship between undulations on the hinge surface to $\delta^{18}O$ maxima from the shell layer above the grey and white growth bands in *C. virginica* from the Pleistocene of Virginia and modern Louisiana fisheries. Andrus and Crowe (2000) sampled carbonate from grey and white growth bands in the hinge cross-section and found a correlation between growth banding and $\delta^{18}O$ maxima in modern *C. virginica* from Georgia. However, a subsequent high-resolution study of the isotopic chemistry of modern *C. virginica* shells from Florida (Surge et al., 2001) sampled carbonate directly from growth bands in the hinge cross-section and documented no correlation among undulations on the hinge surface, growth banding, and $\delta^{18}O$ maxima.

To determine whether a correlation exists between growth banding and $\delta^{18}O$ maxima in *C. virginica,* we build on the approach of Surge et al. (2001) by sampling several years of oyster growth (ranging from 6 to 15 years per individual). We sampled both early and late life history stages, for specimens from a different latitudinal range (e.g., the mid-Atlantic Coastal Plain) with stronger seasonal temperature variability (Kirby et al., 1998). Our study differs from the approaches taken by Kirby et al. (1998) and Andrus and Crowe (2000) in that we collected multiple samples directly from each growth band and distinguished among the morphologies of major (seasonally accreted), disturbance (non-seasonal), and early (non-seasonal) bands (Fig. 2) to explicitly examine the correlation between $\delta^{18}O$ maxima and growth banding. Here, we test the hypothesis that a correlation exists between maxima in subseasonally resolved $\delta^{18}O$ profiles and major grey growth bands in *C virginica* from Pleistocene mid-Atlantic Coastal Plain deposits. Additionally, we assess the importance of sampling density and undertake a review of previous sclerochronological studies of *C. virginica* to determine controls on the ability to detect a relationship between $\delta^{18}O$ values and growth banding.

2. Methods

Bulk samples of oysters were collected from Pleistocene outcrops in both Delaware and Virginia. Shells were sampled from the Omar Formation at two localities in Delaware, Dirickson's Creek (38°29′46.5″N, 75°07′54.9″W) and Pepper Creek (38°31′37.3″N, 75°14′46.4″W) (Ramsey, 2010) (Fig. 3). The Omar Formation consists of dark-grey clayey silt to silty clay deposited in a lagoonal environment with abundant *C. virginica* (Ramsey, 2010).

Amino acid racemization (AAR) estimates constrain the Omar Formation to the middle Pleistocene, with estimates ranging from 400 ka (MIS 11) to 347 ka (MIS 9) (Ramsey, 2010). Virginia samples were collected from the Elsing Green Alloformation at Holland Point (37°30′45.9″N, 76°25′59.9″W) (Fig. 3). The Elsing Green unit, previously part of the Tabb Formation, consists of a basal dark-blue clay that grades upwards into yellow-brown fine to coarse sands, recording a Pleistocene transgression and the transition from a protected estuary to coastal estuary mouth (Berquist et al., 2014; Layou et al., 2016). AAR age estimates place the base of the Elsing Green Formation at MIS 7 or 9 (195–347 ka) (Wehmiller, 2016).

One valve from each site, for a total of three *C. virginica* specimens, was selected for stable isotope geochemical ($\delta^{18}O$ and $\delta^{13}C$) analysis. In keeping with the precedent set by past studies, we analyzed left valves as they provide the largest surface area for sampling and preserve the entire ontogenetic history of the oyster (Kirby et al., 1998). Specimens were selected based on the quality of preservation, absence of bioerosion, and completeness of the hinge. Following the procedures of Andrus and Thompson (2012), valves were bisected down the resilifer, parallel to the greatest axis of growth in order to expose the growth bands in the hinge cross-section (Fig. 1). Valves were thick-sectioned using a low-speed, water-cooled Felker Tile Master saw with diamond tipped blade, then polished using fine-grit sandpaper to create a horizontal plane for sampling. Depending on the size of the hinge, thick-sections were either embedded in epoxy (Buehler Epothin) or affixed to a petrographic slide using Crystalbond thermal adhesive so that the surface closest to the organism's medial plane was exposed for sampling.

Powdered carbonate samples were collected from each shell using a New Wave/Merchantek micromill fitted with a 0.5 mm silicon carbide drill bit and operated using a computer-controlled XYZ micromilling system. Milling paths were drawn within the growth bands themselves, rather than the translucent shell layer above, parallel to the shape of the individual growth bands (Fig. 4). The shape of the milling paths minimized the amount of time-averaging and duplicate sampling within the same growth band and maximized the amount of shell powder produced. We then interpolated additional milling paths between the boundary of each grey and white growth band with a spacing of approximately 200 μm, measured perpendicular to the middle of the previous path (Fig. 4). Each path was milled at the shallowest possible depth (200 μm) to account for the three-dimensional curvature of the shell and to prevent milling into an adjacent white or grey growth band. In specimen AD1, 182 consecutive samples were collected for isotope analysis across the entire shell, producing approximately six samples per millimeter. Specimen PC3 was the smallest shell sampled. Although 60 samples were collected from across the entire shell, only 53 samples were reliably measured due to broken seals on several of the sample bottles, producing approximately six samples per millimeter. For the portion of HP3 that was selected for micro-milling, a total of 115 samples were collected across the sampled portion of the resilifer, or approximately five samples every millimeter. If a milling path occurred on the boundary between growth bands, the sample was assigned to the

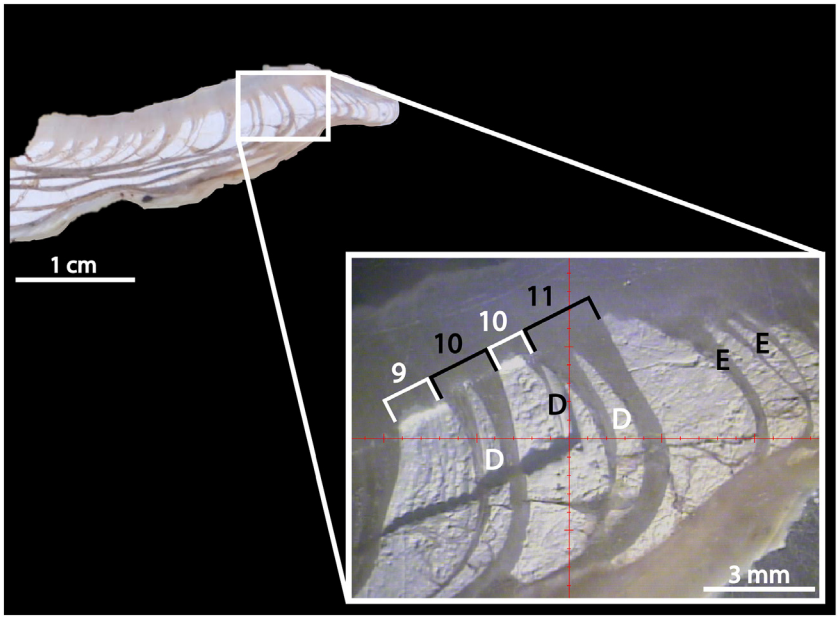

Fig. 2. A close-up of the hinge cross-section for shell AD1 displaying major, disturbance (D), and early growth bands (E). Major white and grey growth bands, marked by white and black brackets labeled 9, 10, and 11, form with seasonal temperature fluctuations. Major grey growth bands 10 and 11 both contain white disturbance bands, marked by a white D. Major white growth band 10 contains a grey disturbance band, marked by a black D. Disturbance bands can be identified if they fail to reach an asymptote in the cross-section, if they fail to make contact with the surficial layer of foliated calcite, or if they contact it at a single point (see major white growth band 10 in the top left quadrant). Major grey growth bands disrupted by a white disturbance band will either coalesce at the initiation of the growth bands or at their asymptote and are counted as a single major growth band (see for example major grey growth bands 10 and 11). Growth bands marked by an E are designated as early grey growth bands (see Discussion Section 4.3). Early grey growth bands may be mistaken for major growth bands during growth band counting; however, these growth bands do not reach the same depth in the resilifer cross-section as the major growth bands, which can only be seen by observing the entire hinge cross-section.

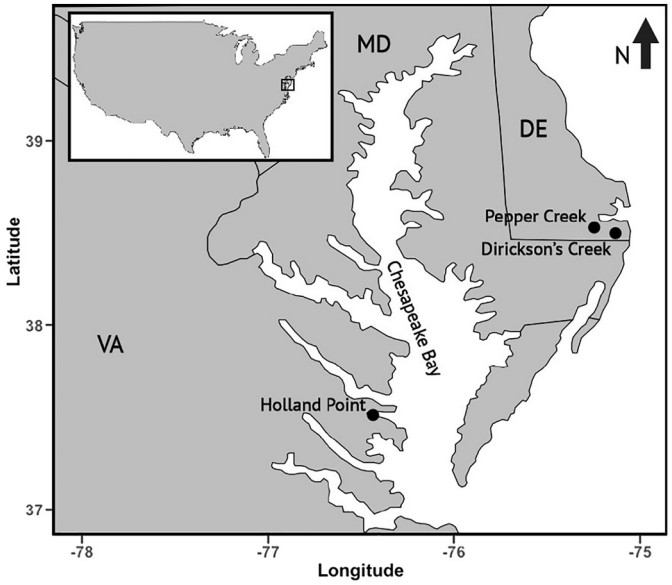

Fig. 3. Map of sampling sites, with inset image of the continental United States. Sampling efforts were focused on the regions surrounding the modern Chesapeake and Delaware Bays to assess the validity of growth band counting for the major fisheries in Virginia, Delaware, and Maryland.

previous colored growth band to avoid bias during data analysis.

We standardized the identification of growth bands by counting grey and white growth bands in the shell cross-section prior to drilling. While similar in mineralogy, the growth bands in *Crassostrea* differ in color due to differences in their microstructure. The grey bands are composed of calcite biominerals arranged into tight sheets (folia), while the white bands are composed of irregularly packed biominerals with spaces between leaflets of biominerals (Checa et al., 2007; Lee et al., 2011; Dauphin et al., 2013). Both materials are structurally similar, with differences in growth rate controlling the orientation of crystal growth (Checa et al., 2018). Previous studies of *C. gigas* (Fan et al., 2011) differentiated between growth bands formed during seasonal temperature fluctuations (major growth bands) and those formed due to sudden environmental changes and other aperiodic causes of growth variation (disturbance bands) by correlating growth bands with undulations on the resilifer surface.

Similar to Surge et al. (2001), we were unable to identify undulations (i.e., concave bottoms and convex tops; Kirby et al., 1998) on the resilifer surface of *C. virginica*. However, we were able to differentiate between major and disturbance bands by using the shape and position of grey and white growth bands in the hinge cross-sections (Fig. 2). If two growth bands of the same color were conjoined at either their initiation beneath the resilifer surface or at their asymptotes in the shell cross-section, the growth bands were counted as the same major growth band, and the growth band between them was counted as a disturbance band (Fig. 2). This was done to minimize the double counting of growth bands and to avoid counting disturbance bands. As we were primarily interested in identifying growth bands due to seasonal temperature changes, disturbance bands were not included in our statistical analysis. For subsequent analyses, we also differentiated between major and early growth bands (Fig. 2). Early growth bands are accreted during fast growth in early ontogeny, thus recording a different seasonal signal than major growth bands, and often fail to reach the same depth in the resilifer cross-section as major growth bands. However, we were unable to differentiate between major and early growth bands with our initial criteria for counting growth bands and thus both were included in our statistical analyses.

Powder samples from each shell were weighed and collected in 4.5 mL round bottomed borosiclicate Exetainer vials. All samples were analyzed at the University of Alabama over the period of 2015–2017 using a Thermo Gas Bench II coupled to a Thermo Delta V isotope ratio mass spectrometer (IRMS) in continuous flow mode. Samples were reacted with orthophosphoric acid at 50 °C to produce CO_2 gas, which was then transferred into the mass spectrometer using a continuous flow of pure helium gas. All stable isotope values are reported in parts per mil (‰) relative to the VPDB standard by correcting to 14 NBS-19 standards per run. NBS-19 was also used to assess and correct for drift and sample size linearity, if indicated. Precision (1σ) was ± 0.10‰ for $\delta^{18}O$ and ± 0.05‰ for $\delta^{13}C$ for first set of runs in 2015, which consisted of the two Delaware specimens, and ± 0.10‰ for $\delta^{18}O$ and ± 0.03‰ for $\delta^{13}C$ for the second set of runs in 2017 for the Virginia specimen.

To ensure a fair and unbiased assessment of the correlation between local $\delta^{18}O$ maxima and growth bands, we detrended each isotope curve. Studies of oysters and other bivalves have found that changes to growth rates and growth patterns in longer-lived organisms distort the $\delta^{18}O$ signal recorded by the shell, creating false trends in annual minima and

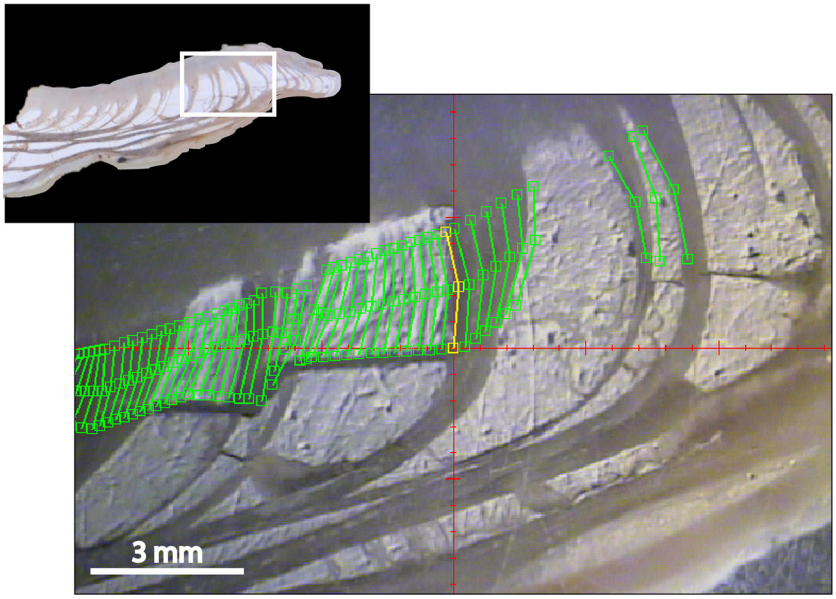

Fig. 4. Part of the hinge cross-section for shell AD1 from the Pleistocene of Delaware, with inset image showing the entire hinge. Milling paths were drawn parallel to the boundaries of the grey and white growth bands (data from full profiles can be found in Fig. 5). Additional transects were then interpolated between the boundary lines to maximize the number of samples collected per growth band.

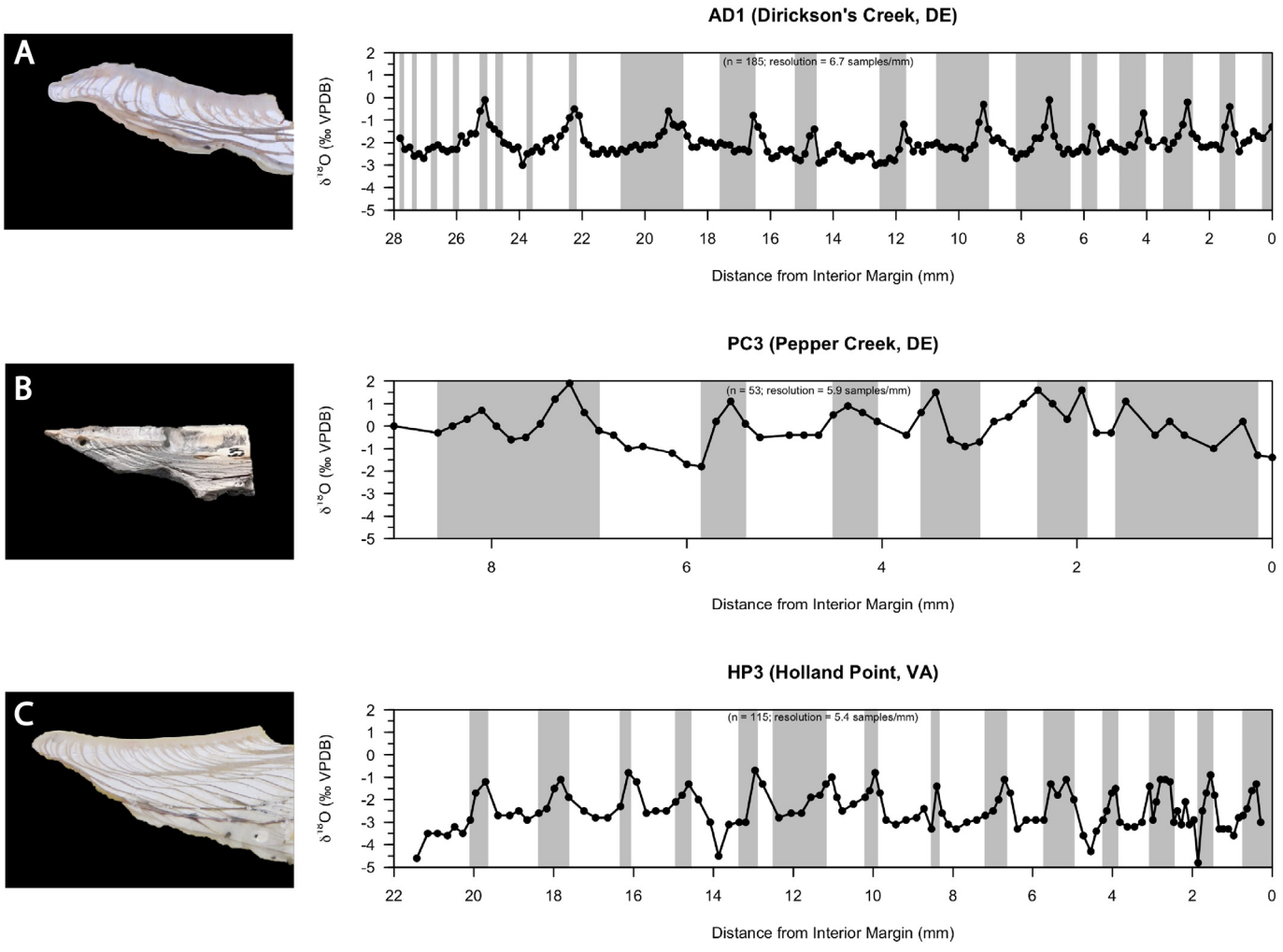

Fig. 5. Detrended $\delta^{18}O$ profiles for each shell sampled are plotted to show seasonal variation in $\delta^{18}O$ values, accompanied by an image of the resilifer cross-section of each shell. Y-axes are identical for all three graphs to show the difference in absolute ranges of each profile. Grey and white boxes on each plot represent the corresponding position of grey and white growth bands in the shell, as counted prior to drilling. In each profile, peak values are found almost exclusively within the major grey growth bands, indicating that major grey growth bands are precipitated during the coldest parts of the year. (A) Isotope profile and corresponding hinge cross-section of shell AD1, from Delaware. (B) Isotope profile and mounted hinge of shell PC3, from Delaware. (C) Isotope profile and hinge cross-section of shell HP3, from Virginia.

maxima (Goodwin et al., 2003). Following Durham et al. (2017), a simple linear regression was run on each dataset to account for ontogenetic changes in growth rates and growth patterns over time by standardizing each $\delta^{18}O$ profile. We were unable to account for trends such as increased periods of reduced growth or growth cessation as these are not fully understood in mid-Atlantic *C. virginica* (Eastern Oyster Biological Review Team, 2007). Once $\delta^{18}O$ profiles were detrended, a basic mathematical criterion was used to determine which data points represented 'peaks' and 'peak values.' The term peak was used to refer to all values on a local part of the $\delta^{18}O$ curve that were one standard deviation above the mean $\delta^{18}O$ value of the profile. The maximum $\delta^{18}O$ value of each peak was referred to as a 'peak value.' Rather than define peaks by comparing local maxima and local means, this method allowed us to focus on regular cyclic oscillations in each $\delta^{18}O$ profile as opposed to the noise created by smaller-scale stochastic variations in temperature and salinity.

3. Results

3.1. AD1 (Dirickson's Creek, Delaware)

For the hinge of AD1, $\delta^{18}O$ values ranged from −3.04‰ to −0.05‰ and $\delta^{13}C$ values ranged from −0.30‰ to +2.00‰ (Fig. S1A) before detrending. Sinusoidal patterns can be seen in both profiles, though cycles are more consistent and regular in the $\delta^{18}O$ profile (Fig. 5A). $\delta^{18}O$ values for the major grey growth bands ranged from −2.93‰ to −0.05‰ before detrending, while the range for major white growth bands was slightly smaller, from −3.04‰ to −0.79‰ (Table 1). On average, 14 samples were collected per each year of growth. A linear regression revealed no significant trend towards increasing or decreasing $\delta^{18}O$ values along the hinge ($\delta^{18}O = -0.005 * \text{Distance} - 1.95$; $R^2 = 0.005$, $p > 0.05$, $n = 182$). We identified 13 peaks in the $\delta^{18}O$ profile, comprising 28 data points or 15% of the entire data set using our criteria for identifying $\delta^{18}O$ peaks. Each peak value was contained within a major grey growth band, and 23 of the 28 data points (82%) sampled from $\delta^{18}O$ peaks occurred within major grey growth bands. The six grey growth bands that did not contain $\delta^{18}O$ peaks were all located towards the distal end of the umbo, representing the earliest growth of the shell.

Table 1
Summary of the measured $\delta^{18}O$ and $\delta^{13}C$ values for each shell before detrending.

		Min	Max	Range	Average
$\delta^{18}O$ (‰ VPDB)					
AD1 (n = 182)	Grey	−2.93	−0.05	2.88	−1.86
	White	−3.04	−0.79	2.25	−2.17
	Total	−3.04	−0.05	2.99	−2.02
PC3 (n = 53)	Grey	−3.22	+0.82	4.04	−0.98
	White	−3.17	+0.19	3.36	−1.63
	Total	−3.22	+0.82	4.04	−1.19
HP3 (n = 115)	Grey	−4.83	−0.69	4.14	−2.04
	White	−4.58	−1.03	3.55	−2.82
	Total	−4.83	−0.69	4.14	−2.43
$\delta^{13}C$ (‰ VPDB)					
AD1 (n = 182)	Grey	−0.03	+2.00	2.03	+0.94
	White	−0.30	+1.33	1.63	+0.57
	Total	−0.30	+2.00	2.30	+0.76
PC3 (n = 53)	Grey	−0.30	+1.40	1.70	+0.61
	White	−0.20	+1.20	1.40	+0.61
	Total	−0.30	+1.40	1.70	+0.61
HP3 (n = 115)	Grey	−1.05	−0.07	0.98	−0.50
	White	−1.95	+0.01	1.96	−0.73
	Total	−1.95	+0.01	1.96	−0.61

3.2. PC3 (Pepper Creek, Delaware)

$\delta^{18}O$ values across the hinge of PC3 ranged from −3.22‰ to +0.82‰, while $\delta^{13}C$ values ranged from −0.30‰ to +1.40‰ (Fig. S1B) before the data were detrended. Peaks in the $\delta^{18}O$ profile are broader than in AD1; however, there is less regularity in the amplitude of $\delta^{18}O$ values and growth band width when compared to the isotope profiles of the other shells (Fig. 5B). Similar to shell AD1, there was some overlap in the range of $\delta^{18}O$ values between the major grey and white growth bands. $\delta^{18}O$ values for the grey growth bands ranged from −3.22‰ to +0.82‰ before detrending, while the range for white growth bands was slightly smaller, from −3.17‰ to +0.19‰ (Table 1). On average, 9 samples were collected per each year of growth. Fitting a linear function to the data shows a significant increase in $\delta^{18}O$ values from the umbo to the growing edge of the resilifer ($\delta^{18}O = -0.178 * \text{Distance} - 0.387$; $R^2 = 0.224$, $p < 0.01$, $n = 53$). After detrending the data, six $\delta^{18}O$ peaks were identified across the entire isotope profile. Nine of the ten data points (90%) sampled from $\delta^{18}O$ peaks were found within major grey growth bands, with one data point occurring on the boundary between a white and major grey growth band. Maximum $\delta^{18}O$ values fall exclusively within the major grey growth bands, with each of the six peak values occurring within a major grey growth band.

3.3. HP3 (Holland Point, Virginia)

$\delta^{18}O$ values in the sampled hinge of HP3 ranged from −4.83‰ to −0.69‰ before the data were detrended. $\delta^{13}C$ values ranged from −1.95‰ to +0.01‰ (Fig. S1C). Growth band width is relatively uniform throughout the sampled section. While there is regular periodicity within the shell between $\delta^{18}O$ maxima and minima, the amplitude of these variations fluctuates throughout the shell with sharp peaks and troughs. Among the three sampled shells, HP3 contains the greatest range in $\delta^{18}O$ values, with peak-to-trough amplitude ranging from 1.32‰ to 3.97‰ (before detrending) across the shell. The range in $\delta^{18}O$ values for the major grey growth bands for HP3 spanned from −4.83‰ to −0.69‰ before detrending, while the range for major white growth bands was slightly smaller, from −4.58‰ to −1.03‰ (Table 1). Despite the similarity between the ranges of $\delta^{18}O$ values for each growth band, there are clear differences in the distribution of $\delta^{18}O$ values between the grey and white growth bands, which show that higher $\delta^{18}O$ values are more frequently found in grey growth bands (Fig. 5C). This is also reflected in the average $\delta^{18}O$ value for each growth band (Table 1). On average, 8 samples were collected per each year of growth. When a linear regression was fitted to the data, no significant trend in $\delta^{18}O$ values throughout the hinge was recorded ($\delta^{18}O = -0.004 * \text{Distance} - 2.01$; $R^2 = 0.001$, $p > 0.05$, $n = 115$). Within the $\delta^{18}O$ profile, 14 peaks were identified. Of these, 13 peak values (93%) are found within major grey growth bands. The other peak value occurs on the boundary between a major white and major grey growth band and was classified as sampled from white growth band in accordance with our methods.

4. Discussion

4.1. Understanding $\delta^{18}O$ peak distributions

To determine whether a relationship exists between major grey growth bands and $\delta^{18}O$ maxima in our profiles, a two-by-two contingency table was created for each shell using growth band color and $\delta^{18}O$ peak presence/absence. A Fisher's exact test was used to test the null hypothesis that there was no association between growth band color and $\delta^{18}O$ peak presence/absence. A highly significant two-tailed p-value of < 0.001 is reported for each shell, indicating that a strong relationship exists between major growth band-color and $\delta^{18}O$ peak presence/absence (AD1: two-tailed $p \leq 0.001$, $\varphi = 0.694$, $n = 182$;

PC3: two-tailed $p \leq 0.001$, $\varphi = 1.0$, n = 53; HP3: two-tailed $p \leq 0.001$, $\varphi = 0.861$, n = 115). For each Fisher's exact test, the phi coefficient of correlation ranged from 0.69 to 1.00, indicating a strong to very strong correlation between growth band color and $\delta^{18}O$ peak presence/absence across all shells.

To determine whether the distribution of $\delta^{18}O$ peaks among the growth bands was significantly different from a null distribution, the total width of the grey and white growth bands was measured through the middle of the hinge cross-section for each shell and divided by the total length of the hinge. This fraction was then multiplied by the number of peaks in the $\delta^{18}O$ profile of each shell to produce a null distribution of peaks between the grey and white growth bands for each shell. A chi-square goodness of fit test was used to compare observed data to theoretical data for grey and white growth bands separately. Shells AD1 ($\chi^2 = 10.4$, $p = 0.001$, n = 20) and HP3 ($\chi^2 = 13.6$, $p < 0.001$, n = 14) showed a significant deviation from the expected values for a random distribution of $\delta^{18}O$ peaks in their major grey bands; however, shell PC3 ($\chi^2 = 3.47$, $p = 0.062$, n = 6) was just above a 5% threshold for significance. Given the sensitivity of chi-square analyses to small sample sizes, it is likely that the low number of growth bands in shell PC3 interfered with this analysis. In contrast, the distribution of $\delta^{18}O$ peaks for the white growth bands in each shell is significantly different from the null hypothesis of a random distribution. Again, the significance of this trend is weaker in PC3 ($\chi^2 = 4.05$, $p = 0.044$, n = 6) than in shells AD1 ($\chi^2 = 10.1$, $p = 0.001$, n = 20) and HP3 ($\chi^2 = 12.6$, $p < 0.001$, n = 14) due to low sample size. In light of these results, we reject the null hypothesis that $\delta^{18}O$ peaks and growth bands are randomly distributed in these hinges and document a significant correlation between $\delta^{18}O$ peaks and grey growth bands in each of the shells.

Despite the non-random distribution of $\delta^{18}O$ peaks among the grey and white growth bands, there is still significant overlap in the range of $\delta^{18}O$ values recorded by the white and grey growth bands, suggesting that $\delta^{18}O$ values of the grey and white growth bands might be difficult to distinguish statistically. Kernel density plots of $\delta^{18}O$ values for each shell show similar ranges for both the grey and white growth bands (Fig. 6). Mann-Whitney U or *t*-tests, when applied to the $\delta^{18}O$ distribution for each shell, reveal a statistically significant difference ($p < 0.05$) between the $\delta^{18}O$ values of the grey and white growth bands (Table 2).

Table 2
Results from the comparison of the measured $\delta^{18}O$ values from major grey and white growth bands. (Two column table).

	Shapiro-Wilks test		Mann-Whitney U		*t*-test	
	p-Value	W	*p*-Value	U	*p*-Value	t
AD1 (n = 182)	< 0.001	0.905	0.006	3180	–	–
PC3 (n = 53)	0.448	0.987	–	–	0.016	−2.52
HP3 (n = 115)	0.007	0.968	< 0.001	750	–	–

4.2. Implications for growth band counting in mid-Atlantic *C. virginica*

The sinusoidal $\delta^{18}O$ profile observed across all three shells (Fig. 5) represents seasonal fluctuations in temperature (Hong et al., 1995; Kirby et al., 1998; Goodwin et al., 2003; Fan et al., 2011). Sharp and well-defined maxima in the profile represent slowed growth during the coldest months of the year or brief periods of growth cessation when temperatures dip below the tolerance levels of *C. virginica* (Kirby et al., 1998). $\delta^{18}O$ minima characterized by wide troughs, such as those seen in the Delaware samples, represent warmer temperatures and faster growth (Fig. 5). Sharper troughs, observed in the $\delta^{18}O$ profile of shell HP3 from Virginia, may represent breaks in growth during the summer months (Surge et al., 2001). Seasonal fluctuation in salinity may increase the amplitude of peaks and troughs in the profiles but is not the primary driver behind the oscillations seen in the profile (Grimm et al., 2017). Smaller excursions in the $\delta^{18}O$ profiles are especially prominent within the white growth bands and capture sudden environmental fluctuations, such as summer rainstorms, that would have changed the $\delta^{18}O$ value of ambient water. In Pleistocene *C. virginica* from the mid-Atlantic U.S., these fluctuations are clearly distinct from the well-defined peaks and troughs in each profile and do not affect the identification of peaks and troughs.

For each shell, the average $\delta^{18}O$ value of the major grey growth bands is significantly different from the average $\delta^{18}O$ value of the major white growth bands, suggesting that they are precipitated during different parts of the year (Table 2). Major grey growth bands record a larger number of more positive $\delta^{18}O$ values (Fig. 6), a trend driven by the presence of $\delta^{18}O$ peaks and peak values in the major grey growth bands. Although accounting for < 15% of the overall $\delta^{18}O$ profile, these more positive values highlight differences in the seasonal accretion of major growth bands. Sharp peaks in the $\delta^{18}O$ profiles of bivalves represent annual minima in temperature or when temperature tolerances are exceeded and provide roughly annual markers that form during coldest months of the year (Kirby et al., 1998; Goodwin et al., 2003; Fan et al., 2011; Andrus, 2012). These data indicate that, in Pleistocene *C. virginica* from the mid-Atlantic United States, major grey growth bands are regularly accreted during the coldest months of the year. Therefore, we propose that counting major grey growth bands, based on our morphological criteria, can be used as a method for determining the biological age of Pleistocene *C. virginica* from the mid-Atlantic United States. In a similar manner, major white growth bands represent accretion during the warmer months of the year, meaning that a single pair of major grey and white growth bands represents a single year of growth.

The presence of disturbance bands provides an additional complication when attempting to count pairs of growth bands to biologically

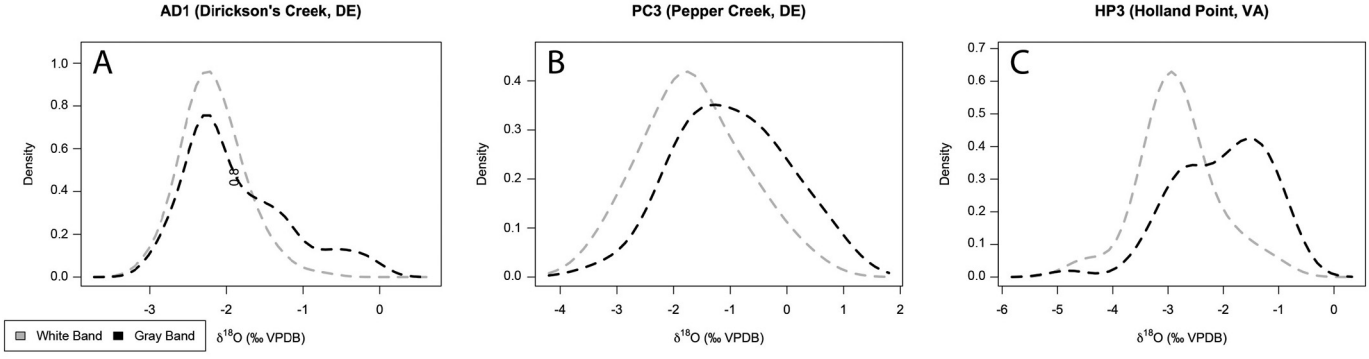

Fig. 6. Kernel density plots of the measured $\delta^{18}O$ values obtained from each sampled shell. (A) Shell AD1 from Dirickson's Creek (DE), (B) shell PC3 from Pepper Creek (DE), and (C) shell HP3 from Holland Point (VA).

age *C. virginica*. For Pleistocene *C. virginica* from the mid-Atlantic Coastal Plain, major grey and white growth bands can be recognized based on whether they reach an asymptote in the shell's cross-section, and whether they reach an asymptote at the same depth as other major growth bands (Fig. 2). Growth bands that fail to reach an asymptote in the cross-section of the shell are classified as disturbance bands and should not be counted for the purpose of determining the lifespan of *C. virginica* from the Pleistocene of the mid-Atlantic Coastal Plain (Fig. 2). White disturbance bands can be further distinguished if they fail to fully contact the layer of foliated calcite above the growth bands (Fig. 2). While disturbance bands are found within major growth bands, they never mark the boundary between major growth bands. Future work is needed to identify the cause of the disturbance bands, and whether these definitions of major grey, major white, and disturbance bands extend to the rest of *C. virginica*'s geographic and stratigraphic range.

4.3. Sampling intensity and the detection of $\delta^{18}O$ peaks within isotope profiles

In addition to understanding the distribution of $\delta^{18}O$ peaks within the isotope profile, we wanted to model the effect of decreased sampling density on our ability to identify a seasonal signal between the major grey and white growth bands. To simulate a decrease in sampling density, we artificially coarsened the resolution of the data collected from shells AD1 and HP3 by taking the average $\delta^{18}O$ values of samples over increasingly wider intervals to generate artificially resampled data sets. We chose to analyze the two largest shells to ensure that each type of major growth band was represented by no fewer than five samples. The averages of every two, three, four, five, and ten data points were calculated for each shell. Each new data set was then analyzed using a Mann-Whitney U or *t*-test to assess the difference between the $\delta^{18}O$ values of both growth bands.

For Pleistocene *C. virginica* from the mid-Atlantic U.S., we find that a minimum sampling density of 3 samples per seasonal cycle is required to detect the original relationship between growth band color and $\delta^{18}O$ values (Fig. 7). Comparing the raw data for shell AD1 to the degraded profiles illustrates that the range between minima and maxima in each $\delta^{18}O$ profile decreases as sampling density decreases, effectively removing the original seasonal signal recorded by the $\delta^{18}O$ of the shell (Fig. 8). While previous studies have highlighted the effect that lower sampling density has on the shape of the isotope profiles recorded in sclerochronological records (e.g. Goodwin et al., 2003; Burchell et al., 2013; West et al., 2018), we would argue that these sorts of sensitivity analyses should be applied to every sclerochronological study to determine optimal sampling strategies. As noted by Burchell et al. (2013), the impact of sampling intensity can vary among ontogenetic ages, environments, geographic regions, and time intervals for the same taxon, as well as among taxa. Here, we quantify the impact that decreasing sampling intensity has on the ability to statistically correlate growth bands to $\delta^{18}O$ peaks.

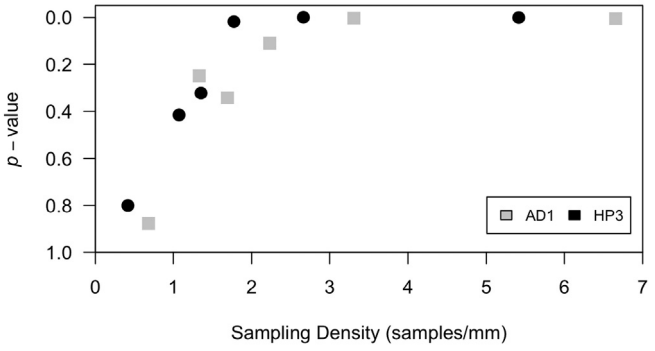

Fig. 7. Simulated resampling of shells AD1 and HP3 at progressively lower sampling densities reveals a decreased ability to distinguish between the $\delta^{18}O$ values of major grey and white growth bands at lower sampling densities. Higher *p*-values at lower sampling densities indicate that the original seasonal profile of the shell is no longer preserved when shells are sampled at a density of fewer than 3 samples per seasonal cycle.

Even when drilling at subseasonal resolutions, a small number of data points per annual cycle may fail to adequately capture the $\delta^{18}O$ signal from the shell. Implementing adaptive sampling strategies (e.g. Fan et al., 2011) and using lower-resolution sampling in growth bands with faster growth may produce artificially smoothed $\delta^{18}O$ profiles and erase interannual variation in the $\delta^{18}O$ signal by reducing the number of data points for each peak and trough in the $\delta^{18}O$ profile. Even in subseasonal sclerochronological studies, greater care must be taken to understand the effects of sampling resolution and its influence on the interpretation of data.

4.4. Factors affecting the correlation between $\delta^{18}O$ peaks and growth bands

Given that studies evaluating the relationship between morphological features and $\delta^{18}O$ maxima (in this study, $\delta^{18}O$ peaks) in *C. virginica* have produced conflicting results (e.g. Kirby et al., 1998; Andrus and Crowe, 2000; Surge et al., 2001; this manuscript), it is important to explore differences in methodology and study system that may explain these disparities. Kirby et al. (1998), Andrus and Crowe (2000), and the current study all found that growth breaks and/or growth bands could be used to biologically age *C. virginica*. In the course of their study, Surge et al. (2001) found no correlation between seasonal $\delta^{18}O$ maxima and the grey growth bands in *C. virginica*, and no significant difference between the $\delta^{18}O$ values of the grey and white growth bands. Kirby et al. (1998), Andrus and Crowe (2000), and Surge et al. (2001) collected modern oysters from estuarine habitats from Louisiana, Georgia, and Florida, respectively, while Kirby et al. (1998) and the current study analyzed Pleistocene oysters from the mid-Atlantic U.S. These four studies all differ somewhat in three important aspects: (1) the lifespan of the oysters examined, (2) sampling of growth bands from early or late life history stages, and (3) study location.

The lifespan of oysters studied affects the strength of the correlation between morphological features and $\delta^{18}O$ maxima when most or all of the hinge is sampled, simply because longer-lived oysters record multiple years for sampling and statistical testing. Modern *C. virginica* tend to be significantly shorter-lived than fossil specimens (Kusnerik et al., 2018), suggesting that lifespan may explain some of the differences documented in these studies. For example, in Kirby et al. (1998), the relationship between convex tops on the resilifer surface and $\delta^{18}O$ maxima is noticeably weaker in modern oysters from Louisiana (2–4 years of growth sampled) than in longer-lived Pleistocene oysters from the Chesapeake Bay (5–6 years of growth sampled). Andrus and Crowe (2000) found a robust correlation between grey growth bands and $\delta^{18}O$ maxima in modern oysters from Georgia, averaging six years of growth sampled per specimen. Surge et al. (2001) tested for a correlation among $\delta^{18}O$ maxima, undulations in the resilifer surface, and grey growth bands of a modern oyster, sampling only two years of growth, and found no evidence to support the findings of Kirby et al. (1998) or Andrus and Crowe (2000). For comparison, if we resample two-year intervals of growth at random from the $\delta^{18}O$ profile of AD1, we consistently fail to find a correlation between $\delta^{18}O$ peaks and grey growth bands (two-tailed $p = 0.4$, $\varphi = 0.707$, n = 31) and $\delta^{18}O$ values and growth band color (Shapiro-Wilks: $p < 0.001$, W = 0.828; Mann-Whitney U: $p = 0.787$, W = 117, n = 31). However, extending our sampling window to six years of growth, similar to specimens in Kirby et al. (1998) and Andrus and Crowe (2000), yields a correlation between $\delta^{18}O$ peaks and growth bands (two-tailed $p = 0.004$, $\varphi = 0.789$, n = 78) and $\delta^{18}O$ values and growth band color (Shapiro-Wilks: $p < 0.001$, W = 0.868; Mann-Whitney U: $p = 0.033$, W = 501, n = 78). Irrespective of the life-span of an oyster, the duration of the sampling window and the number of years sampled plays an important role in documenting the apparent relationship between $\delta^{18}O$ values and

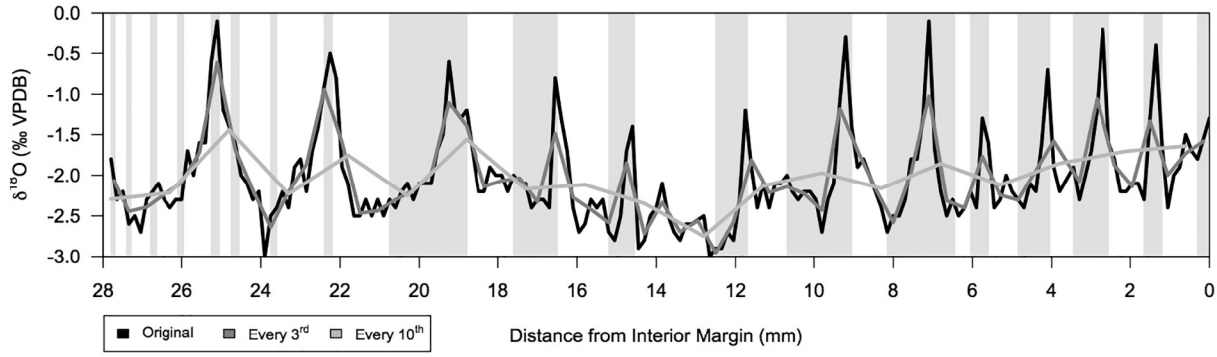

Fig. 8. $\delta^{18}O$ profiles of original and resampled data from shell AD1. As sampling density decreases, the original $\delta^{18}O$ maxima and minima from the shell are obscured or, in some cases, lost completely. Decreasing the number of data points per year, and thus per peak and trough, also changes the position of the minima and maxima in the profile, further obscuring the relationship between $\delta^{18}O$ peaks and growth band color.

growth bands. Longer-lived oysters, such as those sampled by Kirby et al. (1998), Andrus and Crowe (2000), and this study, are preferred when studying the relationship between $\delta^{18}O$ values and morphological features as a larger number of samples spanning several years of growth can be collected.

Preferentially sampling earlier versus later life history stages may also affect the correlation between morphological features and the $\delta^{18}O$ profile. Previous studies have demonstrated the impact that senescence and slowed growth has on the shape and amplitude of $\delta^{18}O$ profile in late life history stages (Goodwin et al., 2003; Goodwin et al., 2010), which could affect the observed correlation between $\delta^{18}O$ and morphological features. Avoiding this complication by sampling the youngest life history stages raises a different set of issues. Pleistocene *C. virginica* from the mid-Atlantic U.S. display grey early growth bands in the youngest portion of the hinge that do not coincide with $\delta^{18}O$ peaks or peak values in the $\delta^{18}O$ profile (Fig. 2). One explanation is that early growth in these oysters is rapid, possibly to prevent predation, and thus grey and white early growth bands are not precipitated annually (Kirby, 2001). Other studies of growth patterns in bivalves have reported similar difficulties in deciphering the relationship between morphological features and isotope profiles during early ontogeny (Richardson et al., 1993; Edie and Surge, 2013; Durham et al., 2017). If we restrict our $\delta^{18}O$ profile for AD1 to its initial two years of growth, similar to the oysters sampled in Surge et al. (2001), we fail to find a correlation between $\delta^{18}O$ peaks and grey growth bands (two-tailed $p = 0.471$, $\varphi = -0.063$, $n = 41$) and $\delta^{18}O$ values and growth band color (Shapiro-Wilks: $p = 0.003$, $W = 0.908$; Mann-Whitney U: $p = 0.595$, $W = 155$, $n = 41$). This would suggest that a correlation between $\delta^{18}O$ peaks and growth band color is absent or difficult to detect during early growth. Further work must be done to understand the nature of these early growth bands, whether they can be differentiated throughout the geographic and stratigraphic ranges of *C. virginica*, and why their pattern of accretion differs from those seen in later stages of oyster growth.

Latitudinal differences in winter temperatures and seasonal temperature ranges may also explain the discrepancies noted in previous studies. Each study, including this manuscript, reports $\delta^{18}O$ values that suggest a similar average summer temperature (around 30 °C); however, Surge et al. (2001) reported average winter temperatures that are 10 °C warmer than Kirby et al. (1998), Andrus and Crowe (2000), and this manuscript. Warmers winters documented by Surge et al. (2001) would diminish the amplitude of seasonal oscillations in $\delta^{18}O$ values, weakening the correlation between $\delta^{18}O$ maxima and grey growth bands. A 20 °C difference in winter and summer temperatures (e.g. Kirby et al., 1998; Andrus and Crowe, 2000) would correspond to a ~5.00‰ range in annual $\delta^{18}O$ values, while a 10 °C difference (e.g. Surge et al., 2001) would only produce a ~2.50‰ difference between winter and summer values (Epstein et al., 1953). Based on these data, growth band counting is most applicable for *C. virginica* specimens collected from environments with higher seasonal temperature differences and colder winters. This would explain why studies conducted at lower latitudes with diminished seasonal temperature fluctuations may find no correlation between growth bands and fluctuations in $\delta^{18}O$ values, while studies conducted at higher latitudes, where there are higher seasonal temperature fluctuations and cooler winter temperatures, document a correlation (for a more general discussion, see Twaddle et al., 2016).

Although we find that seasonal temperature differences are one of the keys to identifying a correlation between growth bands and $\delta^{18}O$ peaks in *C. virginica*, we would caution applying this biological aging technique beyond the mid-Atlantic United States. Many bivalves, including *Mercenaria*, *Phacosoma*, and *Crassostrea*, show changes in growth patterns along latitudinal gradients (Tanabe and Oba, 1988; Jones and Quitmyer, 1996; Schöne et al., 2003; Andrus and Crowe, 2008; Andrus, 2012). In *Mercenaria*, accretion of grey growth bands occurs during the summer at lower latitudes and in the winter at higher latitudes, with a transition zone in between that includes both phenotypes (Jones and Quitmyer, 1996). Tanabe and Oba (1988) documented a decrease in the annual number of growth bands from lower to higher latitudes in *Phacosoma* coinciding with the length of the growing season. The next step in expanding the applicability of growth band counting for biologically aging *C. virginica* would involve subseasonal sclerochronological sampling of *C. virginica* over a wider latitudinal gradient to investigate the scope of this method in assisting conservation efforts.

4.5. Implications of growth band counting for conservation paleobiology of oysters

Pleistocene assemblages provide a much-needed source of baseline data for oysters before human disturbance but gathering population-level data has been hindered by the cost (in both time and money) of using stable isotope sclerochronology to biologically age specimens (Harding et al., 2008; Beck et al., 2011; Durham et al., 2017). The relationship between major grey growth bands and $\delta^{18}O$ peaks in *C. virginica* demonstrates that counting the major growth bands in the resilifer cross-section can be used to biologically age oysters from the Pleistocene of the mid-Atlantic U.S., without collecting stable isotope data from each specimen. Growth band counting is a cost-efficient and repeatable method that would allow conservation paleobiologists to quickly collect large amounts of information from Pleistocene *C. virginica*, including data on life span, growth rates, and population structure. This would open the door to a new understanding of population dynamics in fossil and modern oyster reefs (Jackson et al., 2001; Kraeuter et al., 2007).

Data on ancient populations could also be used to create an ecological baseline for ecologists working to remediate modern ecosystems

(Jackson et al., 2001; Kirby and Miller, 2005; Harding et al., 2008; Beck et al., 2011). Ecological managers have struggled to restore sustainable oyster populations (Harding et al., 2010; Beck et al., 2011) and comparisons between ancient and modern reefs could potentially highlight deficiencies in conservation practices. This study also corroborates techniques used to assess archaeological middens, which could be extended to better understand the fishing practices of ancient American cultures (Andrus, 2011; Blitz et al., 2014; Thompson and Andrus, 2014). In this way, growth band counting could be applied to produce new insight into ancient, colonial, and modern oyster populations, without the need for extensive sclerochronological analyses to biologically age individual oysters.

5. Conclusions

Our results suggest that growth band counting is a reliable method for biologically aging Pleistocene *C. virginica* from the mid-Atlantic Coastal Plain. $\delta^{18}O$ profiles generated from oyster hinges with subseasonal resolution demonstrate that major grey growth bands accrete during the coldest months of the year, and that the time from one major grey growth band to the next represents approximately one year of growth. Major growth bands can be easily discerned from disturbance bands based on the presence and depth of their asymptote in the resilifer cross-section. For future sclerochronological studies in other regions, we recommend utilizing adaptive sampling strategies (Schöne et al., 2005; Fan et al., 2011) to assess the effects of: (1) sampling resolution (i.e., number of samples per year), (2) targeting early versus late life history stages, (3) including oysters that vary in lifespan, and (4) identifying major versus disturbance bands. Controlled aquacultural experiments in long-lived extant oysters may provide the best opportunity for determining the timing of growth bands in early ontogeny. Differences in seasonal temperature ranges (namely colder winters), in addition to methodology, explain the conflicting results of past studies assessing the correlation between hinge morphology and $\delta^{18}O$ values. Growth band counting provides a quick and efficient method for biologically aging oysters in ancient, colonial, and modern populations from the mid-Atlantic U.S.

Supplementary data to this article can be found online at https://doi.org/10.1016/j.palaeo.2018.11.029.

Acknowledgments

We would like to extend a special thanks to K. Ramsey and the Delaware Geological Survey for their help throughout this project, as well as J. Lambert at the University of Alabama stable isotope lab and E. Goddard at University of South Florida isotope Lab. We are grateful to L. Harper and two anonymous reviewers whose comments greatly improved the original manuscript. We thank C. Abbott, E. Dale, K. Merritt, C. Barto, and M. Irwin for their help collecting, processing, and analyzing oysters for this project. We would also like to thank the Roane family for access to Holland Point, Virginia. Funding for the instrumentation at the University of Alabama Stable Isotope Lab used in the project was provided by the National Science Foundation Instruments and Facilities grant number EAR-0949303.

References

Andrus, C.F.T., 2011. Shell midden sclerochronology. Quat. Sci. Rev. 30, 2892–2905.
Andrus, C.F.T., 2012. Isotope sclerochronology in southeastern US archaeology to estimate season of capture. In: Reitz, E.J., Quitmyer, I.R., Thomas, D.H. (Eds.), Seasonality and Human Mobility Along the Georgia Bight. Vol. 97. American Museum of Natural History Anthropological Papers, pp. 123–133.
Andrus, C.F.T., Crowe, D.E., 2000. Geochemical analysis of *Crassostrea virginica* as a method to determine season of capture. J. Archaeol. Sci. 27, 33–42.
Andrus, C.F.T., Crowe, D.E., 2008. Isotope analysis as a means for determining season of capture for *Mercenaria*. In: Thomas, D.H. (Ed.), Native American Landscapes of St Catherine's Island, Georgia. Vol. 88. Anthropological Papers: American Museum of Natural History, pp. 498–518.
Andrus, C.F.T., Thompson, V.D., 2012. Determining the habitats of mollusk collection at the Sapelo Island shell ring complex, Georgia, USA using oxygen isotope sclerochronology. J. Archaeol. Sci. 39, 25–228.
Beck, M.W., et al., 2011. Oyster reefs at risk and recommendations for conservation, restoration, and management. Bioscience 61, 107–116.
Berquist Jr., C.R., Gilmer, A.K., Hancock, G., 2014. The Elsing Green, a new Pleistocene alloformation in the Virginia Coastal Plain. Geol. Soc. Am. Abstr. Programs 46 (3), 82.
Blitz, J.H., Andrus, C.F.T., Downs, L.E., 2014. Sclerochronological measures of seasonality at a Late Woodland mound on the Mississippi Gulf Coast. Am. Antiq. 79, 697–711.
Brocas, W.M., Reynolds, D.J., Butler, P.G., Richardson, C.A., Scourse, J.D., Ridgway, I.D., Ramsay, K., 2012. The dog cockle, *Glycymeris glycymeris* (L.), a new annually- resolved sclerochronological archive for the Irish Sea. Palaeogeogr. Palaeoclimatol. Palaeoecol. 373, 133–140.
Burchell, M., Cannon, A., Hallmann, N., Schwarcz, H.P., Schöne, B.R., 2013. Refining estimates for the season of shellfish collection on the Pacific Northwest Coast: applying high resolution stable oxygen isotope analysis and sclerochronology. Archaeometry 55, 258–276.
Butler, P.G., Schöne, B.R., 2017. New research in the methods and applications of sclerochronology. Palaeogeogr. Palaeoclimatol. Palaeoecol. 465, p, 295–299.
Checa, A.G., Esteban-Delgado, F.J., Rodríguez-Navarro, A.B., 2007. Crystallographic structure of the foliated calcite of bivalves. J. Struct. Biol. 157, 393–402.
Checa, A.G., Harper, E.M., González-Segura, A., 2018. Structure and crystallography of foliated and chalk shell microstructures of the oyster *Magallan*: the same materials grown under different conditions. Sci. Rep. 8, 1–12.
Coen, L.D., Brumbaugh, R.D., Bushek, D., Grizzle, R., Luckenbach, M.W., Posey, M.H., Powers, S.P., Tolley, S.G., 2007. Ecosystem services related to oyster restoration. Mar. Ecol. Prog. Ser. 341, 303–307.
Colonese, A.C., et al., 2017. Shell sclerochronology and stable isotopes of the bivalve *Anomalocardia flexuosa* (Linnaeus, 1767) from southern Brazil: implications for environmental and archaeological studies. Palaeogeogr. Palaeoclimatol. Palaeoecol. 484, 7–21.
Dauphin, Y., Ball, A.D., Castillo-Michel, H., Chevallard, C., Cuif, J., Farre, B., Pouvreau, S., Salomé, M., 2013. *In situ* distribution and characterization of the organic content of the oyster shell *Crassostrea gigas* (Mollusca, Bivalvia). Micron 44, 373–383.
Dietl, G.P., Flessa, K.W., 2011. Conservation paleobiology: putting the dead to work. Trends Ecol. Evol. 26, 30–37.
Durham, S.R., Gillikin, D.P., Goodwin, D.H., Dietl, G.P., 2017. Rapid determination of oyster lifespans and growth rates using LA-ICP-MS line scans of shell Mg/Ca ratios. Palaeogeogr. Palaeoclimatol. Palaeoecol. 485, 201–209.
Eastern Oyster Biological Review Team, 2007. Status Review of the Eastern Oyster (*Crassostrea virginica*): Report to the National Marine Fisheries Service. Northeast Regional Office F/SPO-88, pp. 105.
Edie, S.M., Surge, D., 2013. Deciphering annual growth features in *Chione elevata* shells using isotope sclerochronology. PALAIOS 28, 93–98.
Epstein, S., Buchsbaum, R., Lowenstam, H.A., Urey, H.C., 1953. Revised carbonate-water isotopic temperature scale. Bull. Geol. Soc. Am. 64, 1315–1325.
Fan, C., Koeniger, P., Wang, H., Frechen, M., 2011. Ligamental increments of the mid-Holocene Pacific oyster *Crassostrea gigas* are reliable independent proxies for seasonality in the western Bohai Sea, China. Palaeogeogr. Palaeoclimatol. Palaeoecol. 299, 437–448.
Galtsoff, P.S., 1964. The American oyster *Crassostrea virginica* Gmelin. Fish. Bull. 64, 421–425.
Goodwin, D.H., Schöne, B.R., Dettman, D.L., 2003. Resolution and fidelity of oxygen isotopes as paleotemperature proxies in bivalve mollusk shells: models and observations. PALAIOS 18, 110–125.
Goodwin, D.H., Cohen, A.N., Roopnarine, P.D., 2010. Forensics on the half shell: a sclerochronological investigation of modern biological invasion in San Francisco Bay, United States. PALAIOS 25, 742–753.
Grimm, B.L., Spero, H.J., Harding, J.M., Guilderson, T.P., 2017. Seasonal radiocarbon reservoir ages for the 17th century James River, Virginia Estuary. Quat. Geochronol. 41, 119–133.
Hanke, M.H., Posey, M.H., Alphin, T.D., 2017. The influence of habitat characteristics on intertidal oyster *Crassostrea virginica* populations. Mar. Ecol. Prog. Ser. 571, 121–138.
Harding, J.M., Mann, R., Southworth, M., 2008. Shell length-at-age relationships in James River oysters (*Crassostrea virginica*) collected four centuries apart. J. Shellfish Res. 27, 1109–1115.
Harding, J.M., Mann, R., Southworth, M.J., Wesson, J.A., 2010. Management of the Piankatank River, Virginia, in support of oyster (*Crassostrea virginica*, Gmelin 1791) fishery repletion. J. Shellfish Res. 29, 867–888.
Hong, W., Keppens, E., Nielsen, P., Riet, A., 1995. Oxygen and carbon isotope study of the Holocene oyster reefs and paleoenvironmental reconstruction on the northwest coast of Bohai Bay, China. Mar. Geol. 124, 289–302.
Jackson, J.B.C., et al., 2001. Historical overfishing and the recent collapse of coastal ecosystems. Science 293, 629–637.
Jones, D.S., Quitmyer, I.R., 1996. Marking time with bivalve shells: oxygen isotopes and season of annual increment formation. PALAIOS 11, 340–346.
Kirby, M.X., 2001. Paleoecological differences between Tertiary and Quaternary *Crassostrea* oysters, as revealed by stable isotope sclerochronology. PALAIOS 15, 132–141.
Kirby, M.X., Miller, H.M., 2005. Response of a benthic suspension feeder (*Crassostrea virginica* Gmelin) to three centuries of anthropogenic eutrophication in the Chesapeake Bay. Estuar. Coast. Mar. Sci. 62, 679–689.
Kirby, M.X., Soniat, T.M., Spero, H.J., 1998. Stable isotope sclerochronology of Pleistocene and recent oyster shells (*Crassostrea virginica*). PALAIOS 13, 560–569.
Kraeuter, J.N., Ford, S., Cummings, M., 2007. Oyster growth analysis: a comparison of

methods. J. Shellfish Res. 26, 479–491.
Kusnerik, K.M., Lockwood, R., Grant, A.N., 2018. Using the fossil record to establish a baseline and recommendations for oyster mitigation in the mid-Atlantic U.S. In: Tyler, C.L., Schneider, C.L. (Eds.), Marine Conservation Paleobiology. Springer, pp. 75–103.
Layou, K.M., Lockwood, R., Berquist, C.R., Berquist, P.J., 2016. Transgressive Deposits of the Coastal Plain of Mathews County (Middle Peninsula, Virginia). 46th Virginia Geological Field Conference, Guidebook (32 p.).
Lee, S., Jang, Y., Ryu, K., Chae, S., Lee, Y., Jeon, C., 2011. Mechanical characteristics and morphological effect of complex crossed structure in biomaterials fracture mechanics and microstructure of chalky layer in oyster shell. Micron 42, 60–70.
Mann, R., Southworth, M., Harding, J.M., Wesson, J.A., 2009a. Population studies of the native oyster, *Crassostrea virginica* (Gmelin, 1791), in the James River Virginia, USA. J. Shellfish Res. 28 (p), 193–220.
Mann, R., Harding, J.M., Southworth, M.J., 2009b. Reconstructing pre-colonial oyster demographics in the Chesapeake Bay, USA. Estuar. Coast. Mar. Sci. 85, 217–222.
Moore, H.F., 1897. Oysters and methods of oyster culture. In: Report of the U.S. Commission of Fish and Fisheries. US Government Printing Office, pp. 263–340.
Ramsey, K.W., 2010. Stratigraphy, correlation, and depositional environments of the middle to late Pleistocene interglacial deposits of southern Delaware: Delaware Geological Survey. Bur. Mines Rep. Invest. 76 (43 p).
Richardson, C.A., Collis, S.A., Ekaratne, K., Dare, P., Key, D., 1993. The age determination and growth rate of the European flat oyster, *Ostrea edulis*, in British waters determined from acetate peels of umbo growth lines. J. Mar. Sci. 50, 493–500.
Savarese, M., Walker, K.J., Stingu, S., Marquardt, W.H., Thompson, V., 2016. The effects of shellfish harvesting by aboriginal inhabitants of Southwest Florida (USA) on productivity of the eastern oyster: Implications for estuarine management and restoration. Anthropocene 16, 28–41.
Schöne, B.R., Tanabe, K., Dettman, D.L., Sato, S., 2003. Environmental controls on shell growth rates and $\delta^{18}O$ of the shallow-marine bivalve mollusk *Phacosoma japonicum* in Japan. Mar. Biol. 142, 473–485.
Schöne, B.R., Fiebig, J., Pfeiffer, M., Gleβ, R., Hickson, J., Johnson, A.L.A., Dreyer, W., Oschmann, W., 2005. Climate records from a bivalved Methuselah (Arctica islandica, Mollusca; Iceland). Palaeogeogr. Palaeoclimatol. Palaeoecol. 228, 130–148.
Surge, D., Lohmann, K.C., Dettman, D.L., 2001. Controls on isotopic chemistry of the American oyster, *Crassostrea virginica*: implications for growth patterns. Palaeogeogr. Palaeoclimatol. Palaeoecol. 172, 283–296.
Tanabe, K., Oba, T., 1988. Latitudinal variation in shell growth patterns of *Phacosoma japonicum* (Bivalvia: Veneridae) from the Japanese coast. Mar. Ecol. Prog. Ser. 47, 75–82.
Thompson, V.D., Andrus, C.F.T., 2014. Evaluating mobility, monumentality, and feasting at the Sapelo Island Shell Ring Complex. Am. Antiq. 76, 315–343.
Twaddle, R., Ulm, S., Hinton, J., Wurster, C.M., Bird, M.I., 2016. Sclerochronological analysis of archaeological mollusk assemblages: methods, applications, future prospects. Archaeol. Anthropol. Sci. 8, 359–379.
Wehmiller, J., 2016. Aminostratigraphic results and “preliminary” interpretation for Mitchem Pit and Holland Point sties, Virginia. In: Layou, K.M., Lockwood, R., Berquist, C.R., Berquist, P.J. (Eds.), Transgressive Deposits of the Coastal Plain of Mathews County (Middle Peninsula, Virginia): 46th Virginia Geological Field Conference, pp. 27–29.
West, C.F., Burchell, M., Andrus, C.F.T., 2018. Molluscs and paleoenvironmental reconstruction in island and coastal settings: variability, seasonality, and sampling. In: Giovas, C.M., LeFebre, M.J. (Eds.), Zooarchaeology in Practice: Case Studies in Methodology and Interpretation in Archaeofaunal Analysis. Springer, Cham, Switzerland, pp. 191–208.
Zimmt, J.B., Lockwood, R., Andrus, C.F.T., Herbert, G.S., 2016. Revisiting growth increment counting as a method for biologically aging *Crassostrea virginica* from the U.S. Geol. Soc. Am. Abstr. Programs 48 (7), 212.